

## Direct Synthesis of CdSe Nanoparticles in Poly(3-hexylthiophene)

Smita Dayal,\* Nikos Kopidakis, Dana C. Olson, David S. Ginley, and Garry Rumbles

National Renewable Energy Laboratory, 1617 Cole Boulevard, Golden, Colorado 80401

Received August 10, 2009; E-mail: smita.dayal@nrel.gov

Photovoltaic solar cells with an active layer composed of a conjugated polymer and colloidal quantum dots (QDs) are very attractive, as they take advantage of the tunability of the photo-physical properties of the QDs, while retaining the solution processability offered by the polymer. In these cells, photoexcitation takes place primarily in the polymer and generates a strongly bound exciton that can be efficiently dissociated at the interface between the polymer and the QD, provided the electron affinity of the latter is higher.<sup>1</sup>

In this configuration the polymer–QD interface plays a very important role, and it has been shown that when the QDs are capped with organic aliphatic ligands, such as trioctylphosphine oxide (TOPO), efficient electron transfer from the photoexcited polymer to the nanoparticles does not occur.<sup>2</sup> Pyridine treatment is therefore necessary to remove the TOPO and enhance charge transfer. However, the pyridine concentration should be controlled carefully in the polymer–nanoparticle solutions as pyridine is a nonsolvent for the polymer and flocculation of the poly(3-hexylthiophene) (P3HT) chains in an excess of pyridine may lead to the large-scale phase separation resulting in poor photovoltaic device performance.<sup>2</sup> An ideal situation is where the effects of the capping ligand on charge exchange are eliminated and the step of transferring QDs to the polymer solution can be bypassed, achieving direct synthesis of uncapped nanoparticles inside the polymer. Watt et al.<sup>3</sup> have successfully demonstrated the synthesis of PbS dots and rods in a polymer-containing solution, but a similar method cannot be employed for the synthesis of CdSe QDs due to poor precursor solubility and inferior crystal structure obtained at the low reaction temperature. There have been some reports<sup>4</sup> of direct synthesis of CdSe QDs in the polymer-containing solution, but these low-temperature synthetic procedures yield QDs with a wide size distribution.

In this report we employ a high boiling point solvent, 1-octadecene (ODE), for the synthesis of good quality CdSe QDs in a P3HT solution. This synthetic procedure yields homogeneously dispersed CdSe QDs without any indication of phase separation. These nanoparticle–P3HT composites can be dissolved in all common solvents for the polymer, from which thin films can be readily cast. Time-resolved microwave conductivity (TRMC) measurements in these films show that photoinduced charge separation occurs at the interface between the QDs and the polymer, indicating this is a promising approach to the fabrication of efficient QD/polymer hybrid photovoltaic devices.

In a typical synthesis, 9 mg of P3HT (Rieke metals) were dissolved in 1 mL of trichlorobenzene and 3 g of ODE at 260 °C under argon flow. The selenium precursor was made by dissolving 0.5 g of selenium powder (Aldrich) in 63 mL of ODE at 220 °C. Dimethylcadmium was used as a precursor of the cadmium due to the insolubility of other cadmium salts in ODE. Dimethylcadmium is a pyrophoric and explosive reagent and should be handled with extreme caution.<sup>5</sup> A 1:2 ratio of cadmium and selenium precursors in ODE was injected at 260 °C. The reaction solution color

immediately changed to brown from bright orange indicating the formation of CdSe nanoparticles. Nanoparticles were allowed to grow at 230 °C. The reaction mixture was cooled down, and 5 mL of hexane were added at 50 °C. P3HT is insoluble in hexane and therefore results in P3HT precipitation along with the CdSe QDs. The reaction mixture was cleaned by centrifugation.

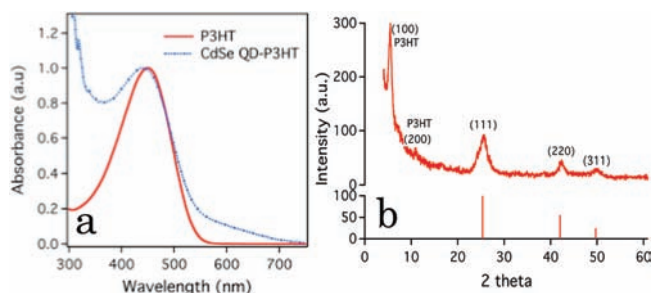


**Figure 1.** (a) Absorption spectra of P3HT in chloroform (red), CdSe QD synthesized in P3HT in chloroform (blue). (b) XRD pattern of CdSe synthesized in P3HT. JPCDS card # 19-0191 for cubic CdSe structure is inserted for reference.

The absorption spectra of pure P3HT and CdSe–P3HT in chloroform are shown in Figure 1a. The spectrum of P3HT in solution shows a characteristic wide peak in the range 300–570 nm with a maximum at 451 nm that can be attributed to the excitons on isolated P3HT chains.<sup>6</sup> For the CdSe–P3HT composite solution, the absorption spectrum exhibits a tail extending out to 700 nm as well as significant absorption at wavelengths shorter than 350 nm. These features that lie outside the primary absorption band of P3HT indicate the presence of CdSe nanoparticles. An excess of P3HT in solution and a high extinction coefficient of P3HT make it difficult to resolve any representative CdSe absorption features. A blank reaction of P3HT without any added CdSe precursors was carried out to understand the effect of reaction temperature on P3HT stability, and based on absorption measurements no degradation of P3HT was observed.

Figure 1b shows the X-ray diffraction (XRD) pattern along with the JCPDS card # 19-0191 for a cubic CdSe structure. All observed peaks can be assigned either to P3HT or to a cubic CdSe lattice structure. The intense peak at  $2\theta = 5.4^\circ$  corresponds to P3HT crystallites and originates from the *a*-axis orientation where the polymer backbone is parallel to the substrate and the plane of the thiophenes is perpendicular.<sup>7</sup> The higher order peak at  $2\theta = 10.9^\circ$  can also be seen. The rest of the diffraction peaks can be assigned to (111), (220), and (311) planes corresponding to the cubic structure of CdSe confirming the high crystallinity of the nanoparticles.

Transmission electron micrograph (TEM) images of the synthesized QDs are shown in Figure 2. Similar to a standard nanoparticle synthesis,<sup>5</sup> reaction temperature plays a significant role in controlling the size and shape of the QDs. TEM images a and b show the QDs synthesized at 200 °C. This synthesis resulted in a wide size

distribution of the nanoparticles, and not all the particles are spherical in shape. Synthesis carried out at 260 °C yields homogeneously dispersed spherical nanoparticles in P3HT as shown in Figure 2c and d. The selected area electron diffraction pattern confirms the high crystallinity of the CdSe. When synthesized at 260 °C 70% of the nanoparticles have a diameter in a range of  $5.5 \pm 0.2$  nm based on a randomly selected sample of 150 nanoparticles.

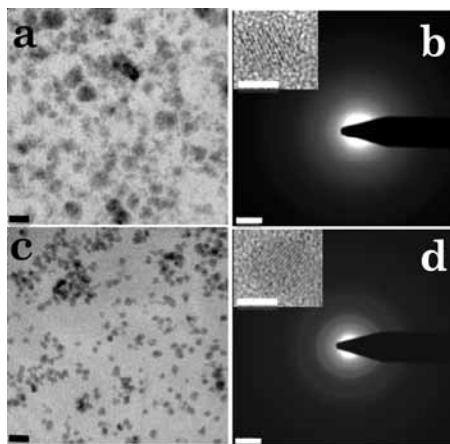


**Figure 2.** (a and c) TEM images of QDs synthesized at 200 and 260 °C, respectively (scale bar 20 nm). (b and d) Corresponding selected area electron diffraction patterns. Insets show the high-resolution TEM images (scale bar 5 nm).

In surfactant-assisted synthesis, nanoparticle growth is controlled by electrostatic interactions and by steric hindrance induced by the surfactant functional group and surfactant side alkyl chains, respectively. P3HT provides a combination of both effects as it contains an electron donating sulfur functionality, a potential anchorage for the nucleation, and growth of nanoparticles along with steric hindrance due to long hexyl side chains as observed by Liao et al.<sup>8</sup> A control reaction carried out in the absence of P3HT results in immediate precipitation of bulk CdSe indicating the role of P3HT in nanoparticle synthesis.

We investigated the charge generation and transfer dynamics in QD–P3HT composite films with the TRMC technique. In TRMC, the transient change in microwave power,  $\Delta P$ , after excitation with a 500 nm, 5 ns laser pulse is directly related to the transient photoconductance,  $\Delta G$ , of the sample by  $\Delta P/P = -K\Delta G$ , where  $K$  is an experimentally determined calibration factor derived from the resonance characteristics of the cavity and the dielectric properties of the sample.<sup>9</sup> The peak photoconductance signal is proportional to the product of the quantum yield for mobile carrier generation per absorbed photon,  $\varphi$ , and the sum of their mobilities,  $\Sigma\mu$ , by  $\Delta G_{\max} = I_0 F_A \beta q_e \varphi \Sigma\mu$ .<sup>10</sup> Here  $I_0$  is the incident photon flux,  $F_A$  is the fraction of incident light absorbed by the sample,  $\beta$  is the ratio between broad and narrow inner dimension of the waveguide,<sup>10</sup> and  $q_e$  is the elementary charge. Figure 3 shows representative photoconductance transients, normalized by absorbed photon flux, for a pure P3HT film and a CdSe–P3HT composite film spun cast from a solution prepared as described above. The enhanced photoconductivity of the composite film (observed over all excitation intensities from  $10^{13}$  to  $5 \times 10^{15}$  photon/cm<sup>2</sup>/pulse) indicates photoinduced charge separation occurs resulting in (a) an increase

of the yield for free carrier generation,  $\varphi$ , in the composite compared to the pure polymer<sup>10</sup> and (b) a higher sum of the mobilities of free carriers because of the contribution of the electron mobility in the CdSe.<sup>11</sup>

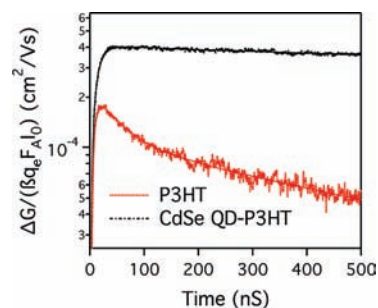


**Figure 3.** Transient photoconductance of CdSe–P3HT (black) and P3HT (red) films upon excitation with 500 nm wavelength, normalized for absorbed photon flux (see text). The incident photo flux was  $10^{14}$  cm<sup>-2</sup>.

Charge separation will also result in longer photocarrier lifetimes due to the electron and the hole residing in two different phases in the composite material,<sup>9</sup> consistent with the data of Figure 3. Indeed, the average decay time for the CdSe–P3HT sample is 79  $\mu$ s with no fast ns decay time components, as opposed to a 10  $\mu$ s average decay time in the pure P3HT sample where ns characteristic times strongly contribute.

In conclusion, we have demonstrated the successful synthesis of CdSe nanoparticles in a P3HT-containing solution with no need for additional surfactant. TRMC studies show photoinduced charge separation at the nanoparticle–polymer interface, which is desired for high efficiency photovoltaic solar cells.

**Acknowledgment.** The authors would like to thank Andrew Norman for TEM microscopy. The Department of Energy EERE Solar Technology Program through the National Center for Photovoltaics Seed Fund Program is acknowledged for funding.

## References

- (1) (a) Greenham, N. C.; Peng, X.; Alivisatos, A. P. *Phys. Rev. B* **1996**, *54*, 17628. (b) Ginger, D. S.; Greenham, N. C. *Phys. Rev. B* **1999**, *50*, 10622. (c) Ginger, D. S.; Greenham, N. C. *Synth. Met.* **1999**, *101*, 425.
- (2) (a) Huynh, W. U.; Dittmer, J. J.; Alivisatos, A. P. *Science* **2002**, *295*, 2425. (b) Huynh, W. U.; Dittmer, J. J.; Libby, W. C.; Whiting, G. L.; Alivisatos, A. P. *Adv. Funct. Mater.* **2003**, *13*, 73.
- (3) (a) Watt, A. A. R.; Thomsen, E.; Meredith, P.; Rubinsztein-Dunlop, H. *Chem. Commun.* **2004**, *10*, 2334. (b) Stavrinadis, A.; Beal, R.; Smith, J. M.; Assender, H. E.; Watt, A. A. R. *Adv. Mater.* **2008**, *20*, 3105.
- (4) (a) Sonar, P.; Sreenivasan, K. P.; Maddanimath, T.; Vijayamohan, K. *Mater. Res. Bull.* **2006**, *41*, 198. (b) Mahmoud, W. E.; El-Mallah, H. M. *J. Phys. D: Appl. Phys.* **2009**, *42*, 035502.
- (5) Murray, C. B.; Norris, D. J.; Bawendi, M. G. *J. Am. Chem. Soc.* **1993**, *115*, 8706.
- (6) Rumbles, G.; Samuel, I. D. W.; Murray, K. A.; DeMello, A. J.; Crystall, B.; Moratti, S. C.; Stone, B. M.; Holmes, A. B.; Friend, R. H. *Synth. Met.* **1996**, *76*, 47.
- (7) Prosa, T. J.; Winokur, M. J.; Moulton, J.; Smith, P.; Heeger, A. J. *Macromolecules* **1992**, *25*, 4364.
- (8) Liao, H.-C.; Chen, S.-Y.; Liu, D.-M. *Macromolecules* **2009**, *42*, 6558.
- (9) Kroeze, J. E.; Savenije, T. J.; Vermeulen, M. J. W.; Warman, J. M. *J. Phys. Chem. B* **2003**, *107*, 7696.
- (10) Dicker, G.; de Haas, M. P.; Siebbeles, L. D. A.; Warman, J. M. *Phys. Rev. B* **2004**, *70*, 045203.
- (11) Piris, J.; Kopidakis, N.; Olson, D.; Shaheen, S. E.; Ginley, D. S.; Rumbles, G. *Adv. Funct. Mater.* **2007**, *17*, 3849.

JA9067673